Pis'ma v ZhETF, vol. 87, iss. 10, pp. 611 – 616 © 2008 May 25

Charm of small x neutrino DIS

R. Fiore[1)], *V. R. Zoller*[1)+]

Dipartimento di Fisica, Università della Calabria
and
Istituto Nazionale di Fisica Nucleare, Gruppo collegato di Cosenza,
I-87036 Rende, Cosenza, Italy

[+]*Institute for Theoretical and Experimental Physics, 117218 Moscow, Russia*

Submitted 4 April 2008

Due to the weak current non-conservation the diffractive excitation of charm and strangeness dominates the longitudinal structure function $F_L(x, Q^2)$ of neutrino DIS at small Bjorken x. Based on the color dipole BFKL approach we report quantitative predictions for this effect in the kinematical range of the CCFR/NuTeV experiment. We comment on the relevance of our findings to experimental tests of PCAC.

PACS: 13.15.+g, 24.85.+p

1. Introduction. The neutrino deep inelastic scattering (DIS) at small values of the Bjorken variable $x_{Bj} = Q^2/2m_N\nu$ provides a useful tool for studies of fundamental properties of electro-weak (EW) interactions. In particular, the analysis of neutrino-nucleon cross sections at vanishing four-momentum transfer squared, Q^2, can be used to test the hypothesis of partial conservation of the axial current (PCAC) in the kinematical region of high leptonic energy transfer, ν, [1, 2] (for theoretical introduction see [3]). The partial conservation hypothesis [4] connects via Adler's theorem [5] the longitudinal structure function (LSF) at $Q^2 \to 0$ induced by the light-quark axial-vector current (ud-current) with the on-shell pion-nucleon total cross section,

$$F_L^{ud}(x, Q^2 \to 0) = \frac{f_\pi^2}{\pi}\sigma_\pi(\nu), \qquad (1)$$

where $f_\pi \simeq 130$ MeV is the pion decay constant (see [6] for more discussion on the origin of Eq.(1)). To test the Eq.(1) the structure function $F_2 = F_L + F_T$ measured experimentally is extrapolated down to $Q^2 \to 0$ making use of the fact that the transverse structure function F_T for ud-current vanishes at $Q^2 \to 0$. It is assumed that the contribution of the charmed-strange (cs) current can be neglected. However, in [6] it has been pointed out that the non-conservation of both axial-vector and vector cs currents leads to the abundant production of charm and strangeness at $Q^2 \lesssim m_c^2$ and for ν well above the charm-strangeness mass threshold.

In this communication we analyze the charged current (CC) DIS in the color dipole (CD) representation of the small-x QCD [7, 8] (for the review see [9]) with particular emphasis on the role of charm and strangeness in the nucleon structure probed by longitudinally polarized electro-weak bosons. We quantify the phenomenon of weak current non-conservation in terms of the light cone wave functions (LCWF) of $|c\bar{s}\rangle$ and $|u\bar{d}\rangle$ states in the Fock state expansion for the light cone EW boson. In Adler's regime of $Q^2 \to 0$ the strong un-equality of masses of the charmed and strange quarks manifests its effects and the CD analysis reveals the ordering of dipole sizes

$$m_c^{-2} < r^2 < m_s^{-2} \qquad (2)$$

typical of the DGLAP [10 – 12] approximation. The multiplication of log's like

$$\alpha_S \log(m_c^2/m_s^2)\log(1/x) \qquad (3)$$

to higher orders of perturbative QCD ensures the dominance of the charmed-strange component, F_L^{cs}, of the LSF

$$F_L = F_L^{ud} + F_L^{cs} \qquad (4)$$

already at $x_{Bj} \lesssim 0.01$, in the kinematical domain covered by the CCFR/NuTeV experiment [13]. In presence of charm and strangeness the slope of F_2 at small Q^2 changes dramatically thus complicating the access to genuine PCAC component[2)] of F_2.

2. Dipole cross sections and light-cone density of $c\bar{s}$ states. When viewed in the laboratory frame the neutrino DIS at small x_{Bj} derives from the absorption of the quark-antiquark, $u\bar{d}$ and $c\bar{s}$, Fock components of the light-cone W^+-boson. We focus on the vacuum exchange

[1)] e-mail: fiore@cs.infn.it, zoller@itep.ru

[2)] Different aspects of the CC inclusive and diffractive DIS have been discussed in [14 – 17].

dominated leading $\log(1/x)$ region of $x \lesssim 0.01$ where the contribution of excitation of open charm/strangeness to the absorption cross section for longitudinal ($\lambda = L$) and transverse ($\lambda = T$) W-boson of virtuality Q^2, is given by the color dipole factorization formula [18, 19, 7]

$$\sigma_\lambda(x,Q^2) = \int dz d^2\mathbf{r} |\Psi_\lambda(z,\mathbf{r})|^2 \sigma(x,r). \qquad (5)$$

The interaction of the color dipole of size $\mathbf{r}$ with the target nucleon is described by the CD cross section $\sigma(x,r)$. In the color dipole approach the BFKL-$\log(1/x)$ evolution [20] of $\sigma(x,r)$ is described by the CD BFKL equation of Ref.[21]. For qualitative estimates the Double Leading Log Approximation (DLLA) [10–12] is suitable. Then, for small dipoles [22]

$$\sigma(x,r) \approx \frac{\pi^2 r^2}{N_c}\alpha_S(r^2)\int_{\mu_G^2}^{A/r^2}\frac{dk^2}{k^2}\frac{\partial G(x,k^2)}{\partial \log k^2} \approx \frac{\pi^2 r^2}{N_c}\alpha_S(r^2)G(x,A/r^2), \qquad (6)$$

where $G(x,k^2) = xg(x,k^2)$ is the gluon structure function and $A \simeq 10$ [22]. We use the one-loop strong coupling $\alpha_S(k^2) = 4\pi/\beta_0 \log(k^2/\Lambda^2)$ with $\Lambda = 0.3\,\mathrm{GeV}$ and $\beta_0 = 11 - 2N_f/3$. In the numerical estimates we impose the infrared freezing, $\alpha_S(k^2) \le \alpha_S^{fr} = 0.8$. For large dipoles, $r \gtrsim r_S$, $\sigma(x,r)$ saturates and the saturation scale, r_S, is as follows

$$r_S^2 = A/\mu_G^2, \qquad (7)$$

where $\mu_G = 1/R_c$ is the inverse correlation radius of perturbative gluons. From the lattice QCD studies $R_c \simeq 0.2 - 0.3\,\mathrm{fm}$ [23]. Because R_c is small compared to the typical range of strong interactions, the dipole cross section evaluated with the decoupling of soft gluons gluons, $k^2 \lesssim \mu_G^2$, would underestimate the interaction strength for large color dipoles. In Ref.[24, 25] this missing strength was modeled by a non-perturbative, soft correction $\sigma_{npt}(r)$ to the dipole cross section $\sigma(r) = \sigma_{pt}(r) + \sigma_{npt}(r)$. Specific form of $\sigma_{npt}(r)$ was successfully tested against diffractive vector meson production data [26].

Denoted by $|\Psi_\lambda(z,\mathbf{r})|^2$ in (5) is the light cone density of $c\bar{s}$ states with the c quark carrying fraction z of the W^+ light-cone momentum and $\bar{s}$ with momentum fraction $1-z$. In particular, $|\Psi_L|^2$ in Eq.(5) is the incoherent sum of two terms, the vector, V_L, and the axial-vector, A_L [14, 27],

$$|\Psi_L(z,\mathbf{r})|^2 = |V_L(z,\mathbf{r})|^2 + |A_L(z,\mathbf{r})|^2, \qquad (8)$$

with [14, 27]

$$|V_L(z,\mathbf{r})|^2 = \frac{2\alpha_W N_c}{(2\pi)^2 Q^2} \times \times \Big\{\big[2Q^2 z(1-z) + (m_c - m_s)[(1-z)m_c - z m_s]\big]^2 \times \times K_0^2(\varepsilon r) + (m_c - m_s)^2 \varepsilon^2 K_1^2(\varepsilon r)\Big\}, \qquad (9)$$

$$|A_L(z,\mathbf{r})|^2 = \frac{2\alpha_W N_c}{(2\pi)^2 Q^2} \times \times \Big\{\big[2Q^2 z(1-z) + (m_c + m_s)[(1-z)m_c + z m_s]\big]^2 \times \times K_0^2(\varepsilon r) + (m_c + m_s)^2 \varepsilon^2 K_1^2(\varepsilon r)\Big\}, \qquad (10)$$

where $\alpha_W = g^2/4\pi$ and the weak charge g is related to the Fermi coupling constant G_F,

$$G_F/\sqrt{2} = g^2/m_W^2. \qquad (11)$$

Hereafter, m_c and m_s are the quark and antiquark masses[3)] and ε^2 which controls the transverse size of $c\bar{s}$ and, with obvious substitutions, of $u\bar{d}$ dipoles is as follows

$$\varepsilon^2 = z(1-z)Q^2 + (1-z)m_c^2 + z m_s^2 \qquad (12)$$

The terms proportional to $K_0^2(\varepsilon r)$ and $K_1^2(\varepsilon r)$ describe the quark-antiquark states with the angular momentum $L = 0$ (S-wave) and $L = 1$ (P-wave), respectively. The weak current non-conservation shows up in terms $\propto m_c^2/Q^2$ and m_s^2/Q^2 which dominate both the vector $|V_L|^2$ and axial-vector $|A_L|^2$ density of states at small Q^2. The P-wave component of $|\Psi_L|^2$ arises only due to the current non-conservation.

3. Qualitative estimates. DLLA. The absorption cross sections for longitudinal EW bosons, σ_L, defined by the Eq.(5) can be converted into the structure function F_L,

$$F_L(x,Q^2) = \frac{Q^2}{4\pi^2\alpha_W}\sigma_L(x,Q^2). \qquad (13)$$

Let us start with $F_L^{cs}(x,Q^2)$ at large Q^2. At $Q^2 \gg m_c^2$ the P-wave component of $|\Psi_L|^2$ proportional to $K_1^2(\varepsilon r)$ vanishes approximately as $(m_c^2/Q^2)\log(Q^2/m_s^2)$ and the structure function F_L^{cs} is dominated by the S-wave component represented by the terms $\propto K_0^2(\varepsilon r)$. The asymptotic behavior of the Bessel function, $K_{0,1}(x) \simeq \simeq \exp(-x)\sqrt{\pi/2x}$ makes the $\mathbf{r}$-integration in Eq. (5) rapidly convergent at $\varepsilon r \gtrsim 1$. For $Q^2 \gg m_c^2$, the product $\alpha_S(Q^2)G(x,Q^2)$ is flat in Q^2. Then, integration over $\mathbf{r}$ yields a broad symmetric z-distribution

[3)] In this paper we deal with constituent quarks in the spirit of Weinberg [28]. The renormalization of the axial charge g_A is neglected here and the ratio g_A/g_V for constituent quarks is assumed to be the same as for current quarks, $g_A = g_V = g$.

$$F_L^{cs} \sim Q^4 \int_0^1 dz \frac{z^2(1-z)^2}{\varepsilon^4} \alpha_S(\varepsilon^2) G(x, A\varepsilon^2) \sim$$
$$\sim \alpha_S(\overline{\varepsilon^2}) G(x, A\overline{\varepsilon^2}), \qquad (14)$$

where $\overline{\varepsilon^2} \sim Q^2/4$ corresponds to the "non-partonic" domain of $z \sim 1/2$. Similar to the LSF of the muon induced DIS (μDIS) [10, 29, 30], the LSF of neutrino DIS (νDIS) is dominated by $r^2 \sim 1/Q^2$ and provides a direct probe of the gluon density $G(x, Q^2)$ [15]. The S-wave component of F_L^{cs} decreases with decreasing Q^2, as shown in Fig.1 by the solid line, but contrary to the μDIS it

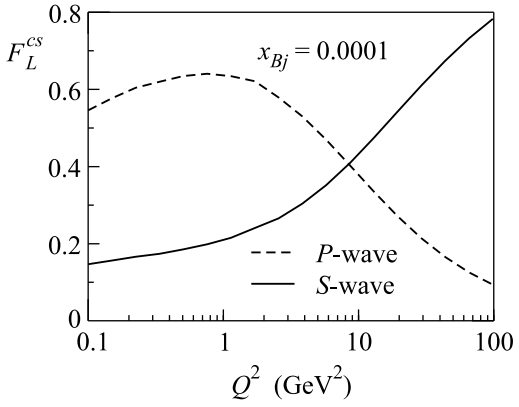

Fig.1. The charm-strange component, $F_L^{cs}(x, Q^2)$, of the longitudinal neutrino-nucleon structure function. Dashed curve corresponds to the P-wave contribution to F_L^{cs}, solid curve represents the S-wave component of F_L^{cs}. The sum of two terms, $F_L^{cs} = P + S$, is a slowly varying function of Q^2

does not vanish at $Q^2 \to 0$ because of the current non-conservation generated by the mass terms in Eqs.(9), (10). Deviations from the symmetric z-distribution do not lead to any sizable effects and F_L^{cs} in Eq.(14) flattens at $Q^2 \sim m_c^2$ (see Fig.1).

At moderate $Q^2 \lesssim m_c^2$ the P-wave component of F_L^{cs} (dashed line in Fig.1) takes over. The P-wave density of $c\bar{s}$ states is more singular at $r \to 0$, $K_1(\varepsilon r) \sim 1/\varepsilon r$. Then, integration over $\mathbf{r}$ in Eq. (5) leads to the z-distribution

$$\frac{dF_L^{cs}}{dz} \sim \frac{m_c^2}{Q^2 z(1-z) + (1-z)m_c^2 + z m_s^2}, \qquad (15)$$

which develops the parton model peaks at $z \to 0$ and $z \to 1$ at asymptotically large Q^2. At $Q^2 \lesssim m_c^2$ the z-distribution becomes highly asymmetric, only the peak at $z \to 1$ survives,

$$\frac{dF_L^{cs}}{dz} \sim \frac{1}{1 + \delta - z}, \qquad (16)$$

where $\delta = m_s^2/(m_c^2 + Q^2)$, so that the charmed quark carries a fraction $z \sim 1 - \delta$ of the W^+'s light-cone momentum. With the Eq.(16) the origin of $\log(m_c^2/m_s^2)$ in (3) becomes evident.

To clarify the issue of relevant dipole sizes one can integrate first over z

$$F_L^{cs} \sim \frac{2N_c}{(2\pi)^3} m_c^2 \int_0^1 dz \int_0^{1/\varepsilon^2} \frac{dr^2}{r^2} \sigma(x, r) \sim$$
$$\sim \frac{2N_c}{(2\pi)^3} \frac{m_c^2}{m_c^2 + Q^2} \int_{1/(m_c^2+Q^2)}^{1/m_s^2} \frac{dr^2}{r^4} \sigma(x, r), \qquad (17)$$

where the factor 2 is due to the additivity of V and A components of F_L^{cs}. For numerical estimates we note that at $x \sim 0.01$ and moderate Q^2 the Born approximation (the two-gluon exchange) gives the results which are not unreasonable phenomenologically [7]. For small dipoles the 2g-exchange yields $\sigma(r) \sim \pi C_F \alpha_S^2 r^2 \log(r_S^2/r^2)$ and the interpolating function is

$$\sigma(r) \sim \pi C_F \alpha_S^2 r^2 \log\left(1 + r_S^2/r^2\right). \qquad (18)$$

Then, for the charmed-strange component of F_L one gets

$$F_L^{cs} \sim \frac{N_c C_F}{4} \frac{m_c^2}{m_c^2 + Q^2} \frac{1}{2!} L^2, \qquad (19)$$

where

$$L = \frac{\alpha_S}{\pi} \log\left(\frac{m_c^2 + Q^2}{m_s^2}\right). \qquad (20)$$

Here, m_s^2 introduces the infrared cutoff and stands, in fact, for $\max\{m_s^2, r_S^{-2}\}$ where r_S^{-2} comes from Eq.(7). In our numerical estimates the constituent strange quark mass equals to $m_s = 0.3\,\text{GeV}$ and is close to r_S^{-1}.

There is also a contribution to F_L^{cs} from the region $0 < r^2 < (m_c^2 + Q^2)^{-1}$:

$$F_L^{cs} \sim \frac{2N_c}{(2\pi)^3} m_c^2 \int_0^1 dz \int_0^{1/(m_c^2+Q^2)} \frac{dr^2}{r^2} \sigma(x, r) \sim$$
$$\sim \frac{N_c C_F}{4} \frac{m_c^2}{m_c^2 + Q^2} \left(\frac{\alpha_S}{\pi}\right)^2 \log\left[r_S^2(m_c^2 + Q^2)\right], \qquad (21)$$

which is short of one log, though. Notice the DLLA ordering of sizes

$$(m_c^2 + Q^2)^{-1} < r^2 < r_S^2, m_s^{-2}, \qquad (22)$$

announced in (2) and elucidated by Eqs.(17), (21).

The rise of $F_L(x, Q^2)$ towards small x is generated by interactions of the higher Fock states, $c\bar{s}$ + gluons, of the light-cone W-boson. Making use of the technique developed in Ref.[7] one can estimate the leading contribution to F_L^{cs} associated with the Fock state $c\bar{s}$ +one gluon. The result is

$$\delta F_L^{cs} \sim \frac{N_c C_F C_A}{4} \frac{m_c^2}{m_c^2 + Q^2} \log\left(\frac{x_0}{x}\right) \frac{1}{3!} L^3, \qquad (23)$$

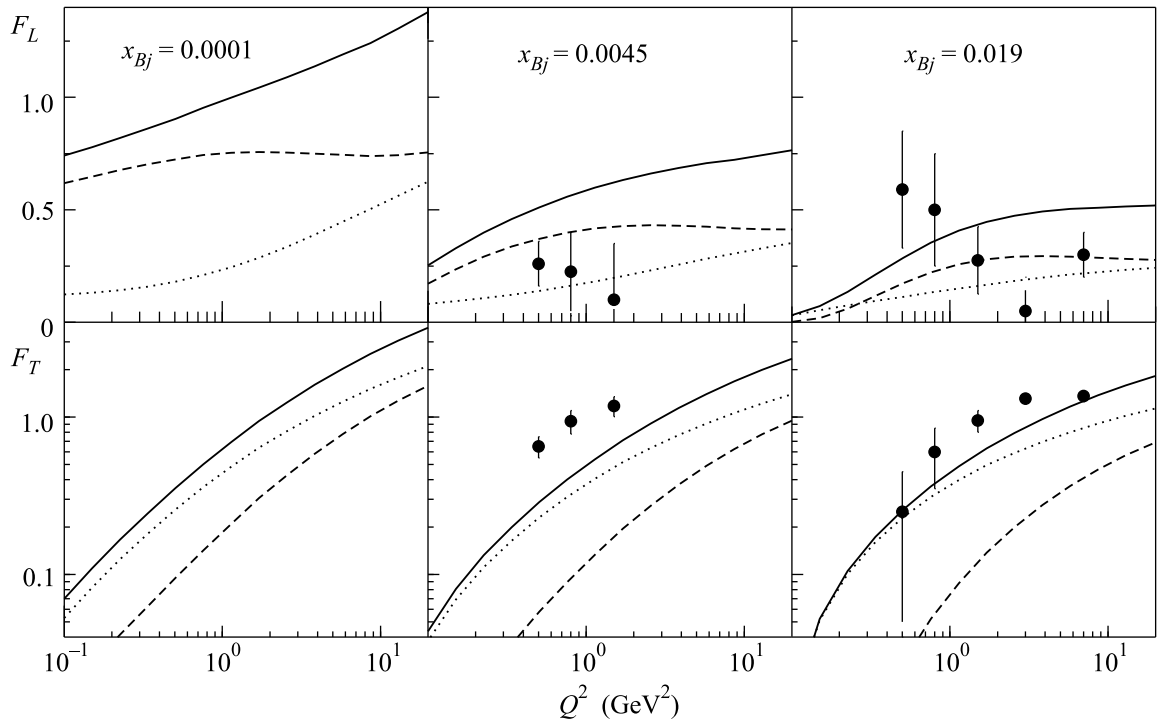

Fig.2. Data points are CCFR measurements of F_L and $F_T = 2xF_1$ [13]. Solid curves show the vacuum exchange contribution to F_L and F_T in νFe interactions. Shown separately are the charm-strange (dashed curves) and light flavor (dotted curves) contributions to F_L and F_T. Also shown are the predictions for F_L and F_T at $x_{Bj} = 10^{-4}$

with $C_A \log(x_0/x)L$ as the DLLA expansion parameter. The slope parameter

$$\Delta = \frac{1}{3} C_A L$$

is rather large, $\Delta \simeq 0.3$ even at $Q^2 = 0$ and we predict a rapid rise of $F_L^{cs}(x, Q^2)$ towards the region of small[4)] x.

Our crude estimate of the P-wave contribution to $F_L^{cs}(x, 0)$ given by Eqs.(20), (21), (23), $F_L^{cs} + \delta F_L^{cs} \simeq 0.4$ at $x \simeq 10^{-4}$ and $x_0 = 0.03$, is compatible with the results of the CD BFKL analysis shown in Fig.1. For comparison, Adler's theorem gives for $F_L^{ud}(x, 0)$ the value $f_\pi^2 \sigma_\pi(\nu)/\pi \simeq 0.30 - 0.35$ and allows only a slow rise of $F_L^{ud}(x, 0)$ with $\nu \propto x^{-1}$,

$$F_L^{ud}(x, 0) \propto (1/x)^{\Delta_{\rm soft}}, \qquad (24)$$

where $\Delta_{soft} \simeq 0.08$ comes from the Regge parameterization of the total πN cross section [31]. Therefore, the charmed-strange current dominates F_L at small-x.

[4)] The DLLA resummation with the infrared cutoff μ_G results in

$$F_L^{cs} \sim \frac{N_c C_F}{4} \frac{m_c^2}{m_c^2 + Q^2} L(m_c^2 + Q^2) \eta^{-1} I_2(2\sqrt{\xi}),$$

where $I_2(z) \simeq \exp(z)/\sqrt{2\pi z}$ is the Bessel function, $\xi = \eta L(m_c^2 + Q^2)$, $L(k^2) = \frac{4}{\beta_0} \log[\alpha_S(\mu_G^2)/\alpha_S(k^2)]$ and $\eta = C_A \log(x_0/x)$.

4. Numerical results and discussion. We evaluate F_L, F_T and F_2,

$$F_2(x, Q^2) = F_L(x, Q^2) + F_T(x, Q^2), \qquad (25)$$

for the νFe and νPb interactions making use of the approach to nuclear shadowing developed in [25]. The $\log(1/x)$-evolution is described by the CD BFKL equation with boundary condition at $x_0 = 0.03$. In order to give a crude idea of finite energy effects at moderately small x we stretch our estimates to $x > x_0 = 0.03$ multiplying the above CD cross sections by the purely phenomenological factor $(1 - x)^5$ motivated by the familiar large-x behavior of DGLAP parameterizations of the gluon structure function of the proton. Here x makes sense of the gluon momentum fraction and equals to $x = x_{Bj}(1 + M^2/Q^2)$ for $Q^2 \lesssim M^2$. For $Q^2 \gtrsim M^2$, $x = 2x_{Bj}$ what corresponds to the collinear DLLA. The mass scale M differs for vector and axial-vector channels, $M = m_\rho, m_{a_1}$ thus introducing non-universality of $\sigma(x, r)$. For charmed-strange states we put $M^2 = 4\,\text{GeV}^2$.

The CCFR Collaboration measurements [13] of the structure function F_L and $F_T = 2xF_1$ as a function of Q^2 for two smallest values of x are shown in Fig.2. From Fig.2 it follows that we strongly overestimate F_L

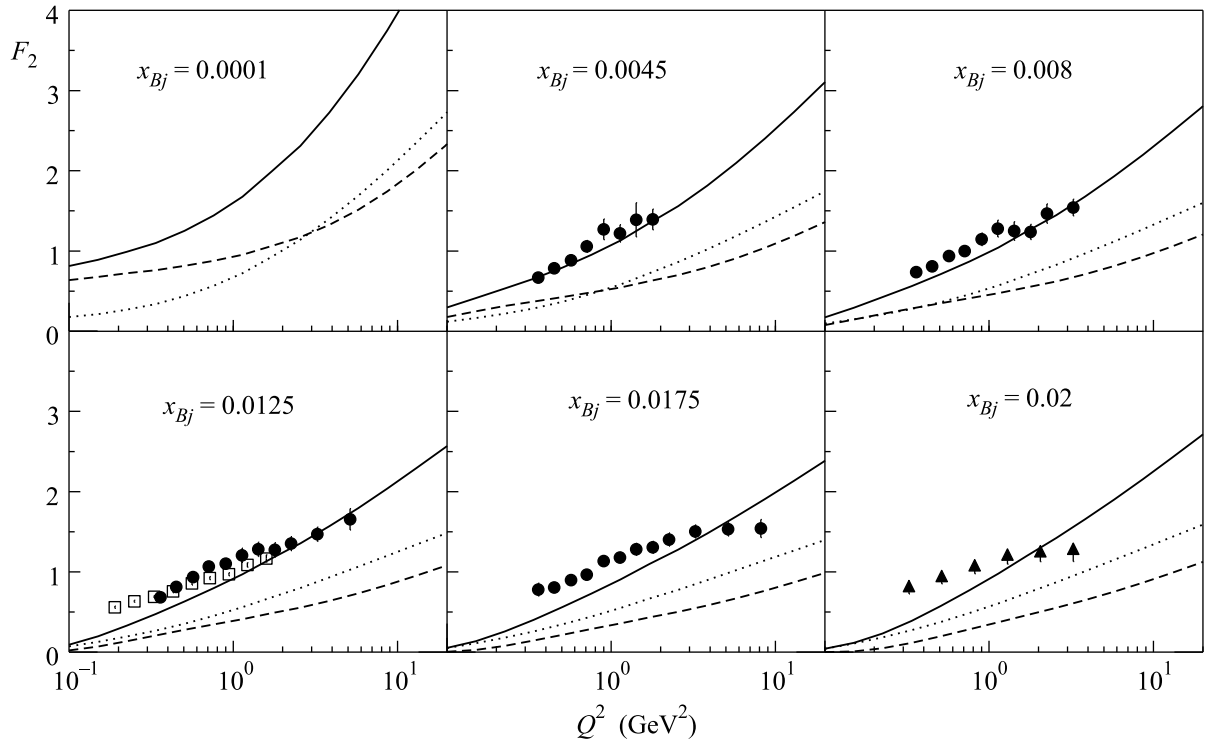

Fig.3. The nucleon structure function $F_2(x, Q^2)$ at smallest available x_{Bj} as measured in νFe CC DIS by the CCFR [2] (circles) and CDHSW Collaboration [33] (squares, $x_{Bj} = 0.015$). Triangles are the CHORUS Collaboration measurements [32] of F_2 in νPb CC DIS. Solid curves show the vacuum exchange contribution to $F_2(x, Q^2)$. Also shown are the charm-strange (dashed curves) and light flavor (dotted curves) components of F_2

and underestimate F_T considerably. However, the sum of two structure functions, $F_2 = F_L + F_T$, shown in Fig.3 is in reasonable agreement with data [2]. Also shown are the high statistics measurement of F_2 from charged current νPb interactions at smallest available $x_{Bj} = 0.02$ by the CHORUS Collaboration [32] and F_2 as measured by the CDHSW collaboration [33] in the νFe DIS at $x_{Bj} = 0.015$ (shown by squares in Fig.3). The cs-component dominates the LSF F_L already at $x_{Bj} = 0.0045$ and affects the slope of both F_L and F_2 at $Q^2 \to 0$. Therefore, the extrapolation of experimentally measured F_2 down to $Q^2 \to 0$ can hardly be used directly to test PCAC. The cs-contribution to F_2 is quite considerable already at $x_{Bj} = 0.0045$ and dominates F_2 at $x_{Bj} = 10^{-4}$ for $Q^2 \lesssim m_c^2$ as shown in Fig.3. The latter observation is important for planned tests of PCAC with high energy neutrino beams.

We underestimate F_2 at moderately small $x \gtrsim 0.01$ and small Q^2 (valence component is not included). Besides, in our analysis of small-x phenomena we rely upon the color dipole factorization (5) which is equally valid for small and large dipoles, in both perturbative and non-perturbative domains. However, two factors in (5) have different status. The CD cross section $\sigma(r) = \sigma_{pt}(r) + \sigma_{npt}(r)$ is corrected for the effects of soft physics while the light-cone density of states $|\Psi_L(r)|^2$ is of purely perturbative nature. Non-perturbative corrections to $|\Psi_L(r)|^2$ at small Q^2 may cause observable effects. In [6] it has been found that the color dipole models successfully tested against the DIS data from HERA underestimate $F_L^{ud}(x, 0)$ defined by the Eq.(1). Particularly, our model with $m_u = m_d = 0.15\,\text{GeV}$ reproduces only half of the empirical value $f_\pi^2 \sigma_\pi / \pi$, not quite bad for the model evaluation of the soft observable, although not satisfactory either. This may lead to the deficit of F_2 in the kinematical region of moderately small x dominated by the ud-current.

It is worth noticing that the nuclear absorption is weaker for charmed-strange states. Therefore, there is a specific nuclear enhancement of the charm production compared to the excitation of light flavors. The analysis of nuclear effects in the CC DIS will be published elsewhere.

5. Summary. We developed the color dipole description of the phenomenon of charged current nonconservation in the neutrino DIS at small Bjorken x. We quantified the effect in terms of the tree level light-cone wave functions and found that the charmed-strange

component of the longitudinal structure function is much larger than its light quark component already at $x \sim$ ~ 0.01. We found also that the excitation of charm and strangeness dominates the structure function $F_2(x, Q^2)$ at $Q^2 \lesssim m_c^2$ and small enough x. A structure function analysis [2, 32, 33] of neutrino DIS data lends support to our predictions.

The authors are indebted to N.N. Nikolaev and B.G. Zakharov for useful comments. V.R.Z. thanks the Dipartimento di Fisica dell'Università della Calabria and the Istituto Nazionale di Fisica Nucleare – gruppo collegato di Cosenza for their warm hospitality while a part of this work was done. The work was supported in part by the Ministero Italiano dell'Istruzione, dell'Università e della Ricerca and by the RFBR grant # 06-02-16905 and # 07-02-00021.

1. G. T. Jones, R. W. L. Jones, B. W. Kennedy et al., Z. Phys. C **37**, 25 (1987).
2. B. T. Fleming, T. Adams, A. Alton et al., Phys. Rev. Lett. **86**, 5430 (2001).
3. B. Z. Kopeliovich and P. Marage, Int. J. Mod. Phys. A **8**, 1513 (1993).
4. Y. Nambu, Phys. Rev. Lett. **4**, 380 (1960); M. Gell-Mann and M. Levy, Nuovo Cimento **17**, 70 (1960).
5. S. Adler, Phys. Rev. B **135**, 963 (1964).
6. R. Fiore and V. R. Zoller, JETP Lett. **85**, 309 (2007).
7. N. N. Nikolaev and B. G. Zakharov, Z.Phys. C **49**, 607 (1991); C **53**, 331 (1992); C **64**, 631 (1994).
8. A. H. Mueller, Nucl. Phys. B **415**, 373 (1994); A. H. Mueller and B. Patel, Nucl. Phys. B **425**, 471 (1994).
9. A. Hebecker, Phys.Rept. **331**, 1 (2000).
10. Yu. L. Dokshitzer, Sov. Phys. JETP **46**, 641 (1977); Yu. L. Dokshitzer, D. I. Dyakonov, and S. I. Troyan, Phys. Rep. C **58**, 265 (1980).
11. V. N. Gribov and L. N. Lipatov, Sov. J. Nucl. Phys. **15**, 438 (1972); L. N. Lipatov, Sov. J. Nucl. Phys. **20**, 181 (1974).
12. G. Altarelli and C. Parisi, Nucl. Phys. B**126**, 298 (1977).
13. U. K. Yang, T. Adams, A. Alton et al., Phys. Rev. Lett. **87**, 251802 (2001).
14. V. Barone, M. Genovese, N. N. Nikolaev et al., Phys. Lett. B **292**, 181 (1992).
15. V. Barone, M. Genovese, N. N. Nikolaev et al., Phys. Lett. B **304**, 176 (1993); B **328**, 143 (1994).
16. V. Barone, M. Genovese, N. N. Nikolaev et al., Phys. Lett. B **268**, 279 (1991); V. Barone, U. D'Alesio, and M. Genovese, Phys. Lett. B **357**, 435 (1995); M. Bertini, M. Genovese, N. N. Nikolaev, and B. G. Zakharov, Phys. Lett. B **442**, 398 (1998); V. Barone, M. Genovese, N. N. Nikolaev et al., Phys. Lett. B **317**, 433 (1993).
17. G. A. Miller and A. W. Thomas, Int. J. Mod. Phys. A **20**,95 (2005); C. Boros, J. T. Londergan, and A. W. Thomas, Phys. Rev. D **58**, 114030 (1998); S. J. Brodsky, I. Schmidt, and Jian-Jun Yang, Phys. Rev. D **70**, 116003 (2004); J. Qiu and I. Vitev, Phys. Lett. B **587**, 52 (2004); S. A. Kulagin and R. Petti, Phys. Rev. D **76**, 094023 (2007); M. B. Gay Ducati, M. M. Machado, and M. V. T. Machado, Phys. Lett. B **644**, 340 (2007).
18. A. B. Zamolodchikov, B. Z. Kopeliovich, and L. I. Lapidus, JETP Lett. **33**, 595 (1981).
19. G. Bertsch, S. J. Brodsky, A. S. Goldhaber, and J. R. Gunion, Phys. Rev. Lett. **47**, 297 (1981).
20. E. A. Kuraev, L. N. Lipatov, and V. S. Fadin, Sov. Phys. JETP **45**, 199 (1977) [Zh. Eksp. Teor. Fiz. **72**, 377 (1977)]; I. I. Balitsky and L. N. Lipatov, Sov. J. Nucl. Phys. **28**, 822 (1978) [Yad. Fiz. **28**, 1597 (1978)].
21. N. N. Nikolaev, B. G. Zakharov, and V. R. Zoller, JETP Lett. **59**, 6 (1994) [Pisma Zh. Eksp. Teor. Fiz. **59**, 8 (1994)].
22. N. N. Nikolaev and B. G. Zakharov, Phys. Lett. B **332**, 184 (1994).
23. M. D'Elia, A. Di Giacomo, and E. Meggiolaro, Phys. Rev. D **67**, 114504 (2003).
24. N. N. Nikolaev and B. G. Zakharov, Phys. Lett. B **327**, 147 (1994); N. N. Nikolaev, B. G. Zakharov, and V. R. Zoller, JETP Lett. **66**, 138 (1997); N. N. Nikolaev, J. Speth, and V. R. Zoller, Phys. Lett. B **473**, (2000) 157.
25. N. N. Nikolaev, W. Schäfer, B. G. Zakharov, and V. R. Zoller, Pis'ma v ZhETF **84**, 631 (2006).
26. J. Nemchik, N. N. Nikolaev, E. Predazzi et al., ZhETF **86**, 1054 (1998).
27. R. Fiore and V. R. Zoller, JETP Lett. **82**, 385 (2005); Phys. Lett. B **632**, 87 (2006).
28. S. Weinberg, Phys. Rev. Lett. **65**, 1181 (1991); Phys. Rev. Lett. **67**, 3473 (1991).
29. A. M. Cooper-Sarkar, G. Ingelman, K. R. Long et al., Z. Phys. C **39**, 281 (1988).
30. R. G. Roberts, *The Structure of the Proton*, Cambridge Univ. Press, 1990, Section 6.4.
31. A. Donnachie and P. V. Landshoff, Phys. Lett. B **296**, 227 (1992).
32. CHORUS Collab., G. Onengut et al., Phys. Lett. B **632**, 65 (2006).
33. CDHSW Collab., P. Berge et al., Zeit. Phys. C **49**, 187 (1991).